J Mol Model (2010) 16:543–550
DOI 10.1007/s00894-009-0557-3

ORIGINAL PAPER

Molecular dynamics studies of a hexameric purine nucleoside phosphorylase

Fernando Berton Zanchi · Rafael Andrade Caceres · Rodrigo Guerino Stabeli · Walter Filgueira de Azevedo Jr.

Received: 20 April 2009 / Accepted: 28 June 2009 / Published online: 11 August 2009

Abstract Purine nucleoside phosphorylase (PNP) (EC.2.4.2.1) is an enzyme that catalyzes the cleavage of N-ribosidic bonds of the purine ribonucleosides and 2-deoxyribonucleosides in the presence of inorganic orthophosphate as a second substrate. This enzyme is involved in purine-salvage pathway and has been proposed as a promising target for design and development of antimalarial and antibacterial drugs. Recent elucidation of the three-dimensional structure of PNP by X-ray protein crystallography left open the possibility of structure-based virtual screening initiatives in combination with molecular dynamics simulations focused on identification of potential new antimalarial drugs. Most of the previously published molecular dynamics simulations of PNP were carried out on human PNP, a trimeric PNP. The present article describes for the first time molecular dynamics simulations of hexameric PNP from *Plasmodium falciparum* (PfPNP). Two systems were simulated in the present work, PfPNP in ligand free form, and in complex with immucillin and sulfate. Based on the dynamical behavior of both systems the main results related to structural stability and protein-drug interactions are discussed.

Keywords Antimalarial drugs · Immucillin · Molecular dynamics · Plasmodium falciparum · Purine nucleoside phosphorylase

F. B. Z and R. A. C. contributed equally to this work, the order of authorship being arbitrary.

F. B. Zanchi · R. G. Stabeli
Programa de Pós Graduação em Biologia Experimental – PGBIOEXP, Universidade Federal de Rondônia, Porto Velho, RO, Brazil

F. B. Zanchi · R. G. Stabeli
IPEPATRO – Instituto de Pesquisa em Patologias Tropicais/ Fundação Oswaldo Cruz - Fiocruz Noroeste, Porto Velho, RO, Brazil

R. A. Caceres · W. F. de Azevedo Jr.
Programa de Pós Graduação em Medicina e Ciências da Saúde, Pontifícia Universidade Católica do Rio Grande do Sul, Porto Alegre, RS, Brazil

R. A. Caceres · W. F. de Azevedo Jr. (✉)
Faculdade de Biociências, Laboratório de Bioquímica Estrutural, Instituto Nacional de Ciência e Tecnologia em Tuberculose, Pontifícia Universidade Católica do Rio Grande do Sul, Porto Alegre, RS, Brazil
e-mail: walter@azevedolab.net

Introduction

Malaria was first reported in the fifth century B.C. by Hippocrates, being one of the oldest human diseases [1]. Current World Health Organization estimates indicate that malaria infection causes 300 million cases of acute illnesses and at least one million deaths yearly [2].

Malaria is caused by the single-celled protozoan parasite, Plasmodium, an organism from the phylum Apicomplexa [3]. Several methodologies have been employed to break the cycle of malaria transmission, such as mosquito control, bed nets, antibiotics, and education, but the lack of reliable employment of these methods has resulted in continued epidemics of malaria [4]. Standard antimalarial drugs such as chloroquine, quinine, amodiaquine, halofantrine, mefloquine, cycloguanil, and pyrimethamine were initially successful, but drug resistance has developed and contributes to the current resurgence of the disease [5].

Purine metabolism in *Plasmodium falciparum* has been proposed as a potential target for antimalarials since it is distinct from that of humans. Plasmodia species are purine auxotrophs; that is, they are not able to synthesize purines *de novo* [6]. To provide purines for nucleic acids synthesis

in the course of cell growth, the *P. falciparum* is dependent on a salvage pathway that employs nucleosides sequestered from the host. PNP is a key enzyme in this pathway (Fig. 1). This enzyme catalyzes the phosphorolysis of inosine to ribose-1-phosphate and hypoxanthine, which is the major purine precursor for salvage pathway [7]. PNP is of pivotal importance for parasite metabolism, which has been demonstrated in studies carried out previously with transition-state analogues that prevent enzyme activity and cause parasite death [8, 9].

Metabolic pathways for purine salvage are significantly distinctive in humans and apicomplexan organisms. The adenosine deaminase and PNP from the *P. falciparum* recognize 5′-methylthionucleosides as favorable substrates, while the respective human enzymes do not [10].

In 2004 the structure of PNP from *Plasmodium falciparum* (PfPNP*)* was determined by X-ray diffraction crystallography. The structure of PfPNP is complexed with sulfate and its natural substrate inosine [11], there is also structural information for the complex with immucillin-H (IMMH), a potent inhibitor of PNP [12], in this context molecular dynamics (MD) simulation can contribute to understanding of structural patterns and biological behavior of proteins under solution condition avoiding the effects of crystal packing over PfPNP. So in the present work we analyzed the structure of PfPNP unbound and in complex with IMMH aiming to identify the structural differences for the substrate interactions in the binding site. The structural features and the structural stability in aqueous solution were assessed by MD simulation. In addition, this is the first report of molecular dynamics simulations for a hexameric PNP, which provides a dynamic view of the protein structure, which can be further employed in cross-docking simulations and structure-based virtual screening.

Materials and methods

Molecular dynamic simulations

The crystallographic structure of PfPNP was retrieved from the Protein Data Bank [13] under access code 1NW4 [12]. This structure is a hexamer (chains A, B, C, D, E, and F) (Fig. 2), the entire protein was used for the simulations because it is biologically functional as a hexamer and the active site is located at the dimer interface.

MD simulations were performed with the GROMACS 3.3.1 [14] package using the Gromos 96.1 (53A6) force field [15]. The IMMH topology file and force field parameters except the charges for inhibitor IMMH were generated by the PRODRG program [16]. The GAMESS program [17], was used for the atomic charges in the IMMH molecule which were submitted to single-point *ab initio* calculations at RHF 6-31G* level in order to obtain Löwdin derived charges. Manipulation of structures was performed with the Swiss-PDBViewer v3.7 program [18]. We simulated two systems. System 1 was composed by the PfPNP stripped of ligands and system 2 was formed by PfPNP in complex with 22 sulfate ions and immucillin-H (PfPNP:IMMH:SO4). Both simulations were run for a time period of 5 ns. In both systems were added Na^+ counter ions using Genion Program of the GROMACS simulation suite in order to neutralize the negative charge density of the systems.

Each structure was placed in the center of a truncated cubic box filled with extended simple point charge (SPC/E) water molecules [19], containing ~56,500 water molecules in both systems. The initial simulation cell dimensions were 9.53 nm×9.31 nm×8.79 nm for both systems, and had the protein solvated by a layer of water molecules in which the minimum distance between the protein surface and the box face was 1.0 nm length in all directions.

During the simulations, bonds lengths within the proteins were constrained by using LINCS algorithm [20]. The SETTLE algorithm was used to constrain the geometry of water molecules [21]. In the MD protocol, all hydrogen atoms, ions, and water molecules were first subjected to 1500 steps of energy minimization by steepest descent followed by 1500 steps of conjugate gradient to remove close van der Waals contacts. The systems were then submitted to a short molecular dynamic with position restrains for a period of 30 ps and afterwards performed a full molecular dynamics without restrains. The temperature of the system was then increased from 50 K to 300 K in 5

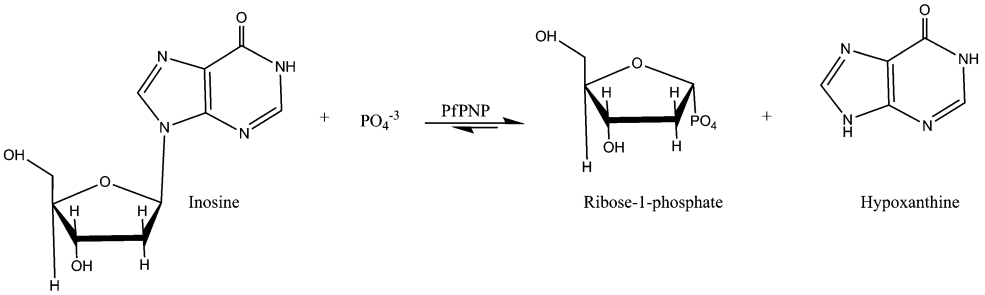

Fig. 1 Phosphorolysis of inosine catalyzed by P. falciparum PNP. The product hypoxanthine is the major precursor for the purine-salvage pathway

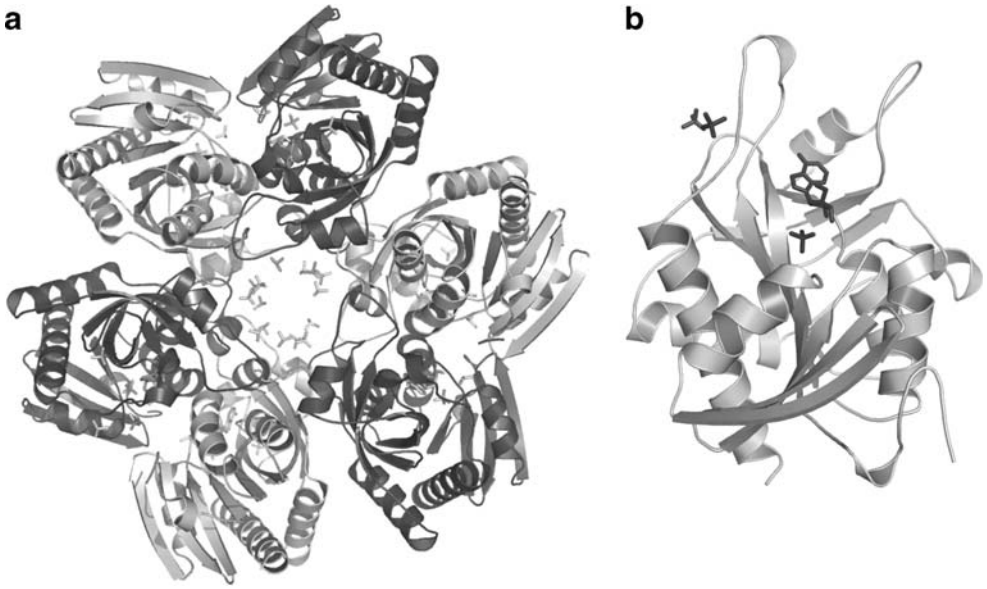

Fig. 2 **a**) Tertiary structure of the homohexamer of PfPNP complexed with IMMH and sulfate ions. **b**) Close-up of PfPNP monomer. The structure is presented as ribbon diagram and IMMH and sulfate ions are presented as stick

steps (50 K to 100 K, 100 K to 150 K, 150 K to 200 K, 200 K to 250 K, 250 K to 300 K), and the velocities at each step were reassigned according to the Maxwell-Boltzmann distribution at that temperature and equilibrated for 10 ps except the last part of thermalization phase that was for 50 ps. Energy minimization and MD were carried out under periodic boundary conditions. The simulation was computed in the NPT ensemble at 300 K with the Berendsen temperature coupling and constant pressure of 1 atm with isotropic molecule-based scaling [22]. The LINCS algorithm, with a 10^{-5} Å tolerance, was applied to fix all bonds containing a hydrogen atom, allowing the use of a time step of 2.0 fs in the integration of the equations of motion. No extra restraints were applied after the equilibration phase. The electrostatic interactions between non-ligand atoms were evaluated by the particle-mesh Ewald method [23] with a charge grid spacing of ~1.0 Å and the charge grid was interpolated on a cubic grid with the direct sum tolerance set to 1.0×10^{-5}. The Lennard-Jones interactions were evaluated using a 1.0 nm atom-based cutoff.

All analyses were performed on the ensemble of system configurations extracted at 0.5 ps time intervals

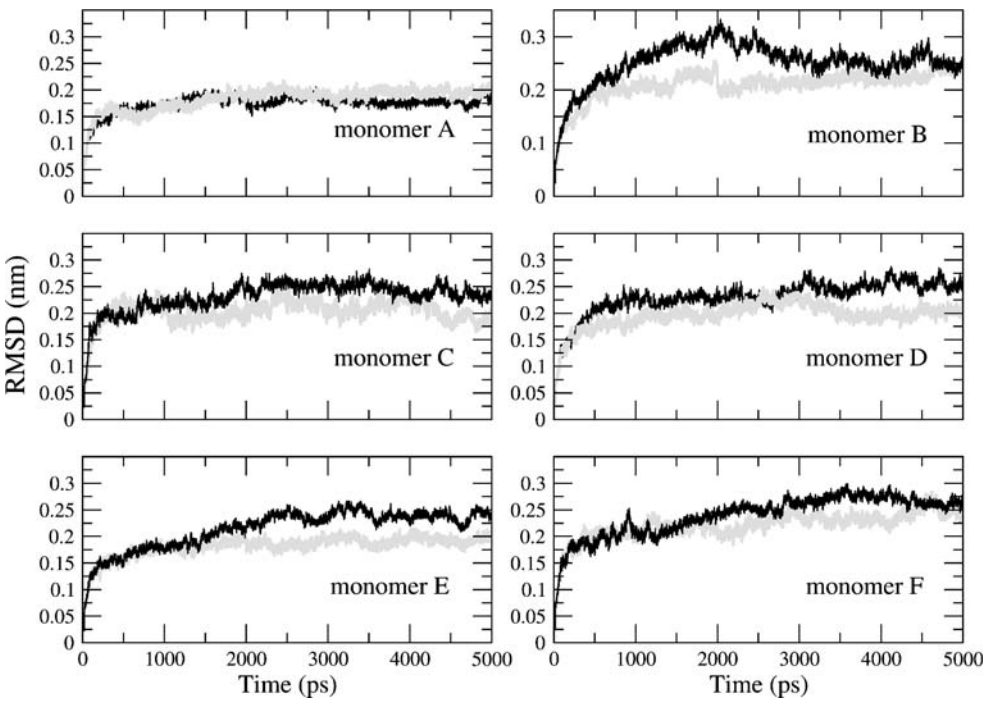

Fig. 3 Graphical representation of root-mean-square deviation (RMSD) of all Cα as a function of time. The black line gives the PfPNP and gray line shows PfPNP:IMMH:SO4 calculation

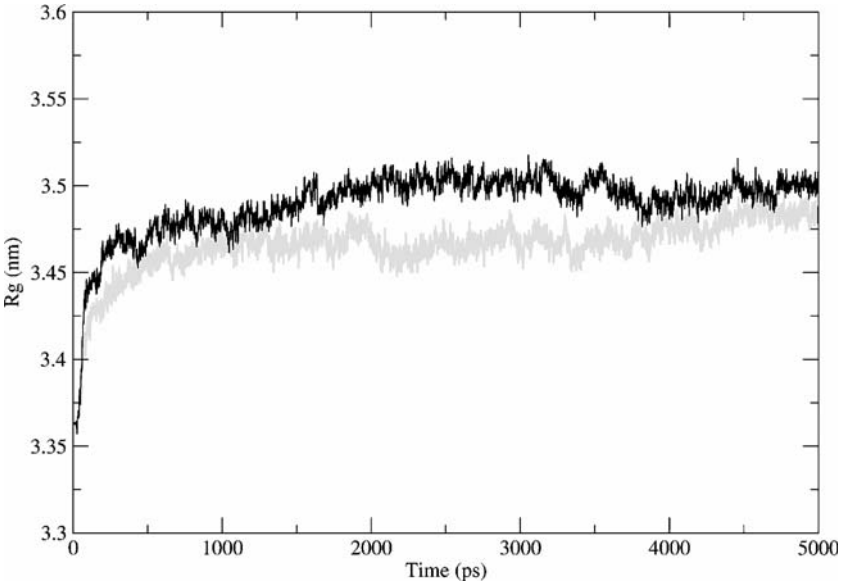

Fig. 4 Radius of gyration of the PfPNP (black line) and PfPNP: IMMH:SO4 (gray line) over simulation

from the simulation and MD trajectory collection was initiated after 1 ns of dynamics to guarantee a completely equilibrated evolution. The MD simulation and results analysis were performed on a DS-Server DuoQuadCore 550 Xeon – 3.00 GHz.

The convergences of the different simulations were analyzed in terms of the secondary structure, radius of gyration (RG), root mean-square deviation (RMSD) from the initial models structures, and root mean-square fluctuation (RMSF).

The RMSFs were calculated relative to the last 4 ns averaged backbone structures, and all coordinate frames from the trajectories were first superimposed on the initial conformation to remove any effect of overall translation and rotation.

Results and discussion

Stability and flexibility of PfPNP and PfPNP:IMMH

Molecular dynamics simulations were carried out for two systems: PfPNP structure in ligand-free form and the complex PfPNP:IMMH:SO4. The main purpose of this study is to elucidate the influence of IMMH on the overall structure of the PfPNP. In order to monitor the progress of PfPNP conformational changes and check the stability of its secondary structure elements during the simulation, we evaluated the root-mean square deviation (RMSD) of the positions for all backbone C-alpha atoms as a function of simulation time. As we can see in Fig. 3, the overall structures were stable along the MD simulations. Analysis

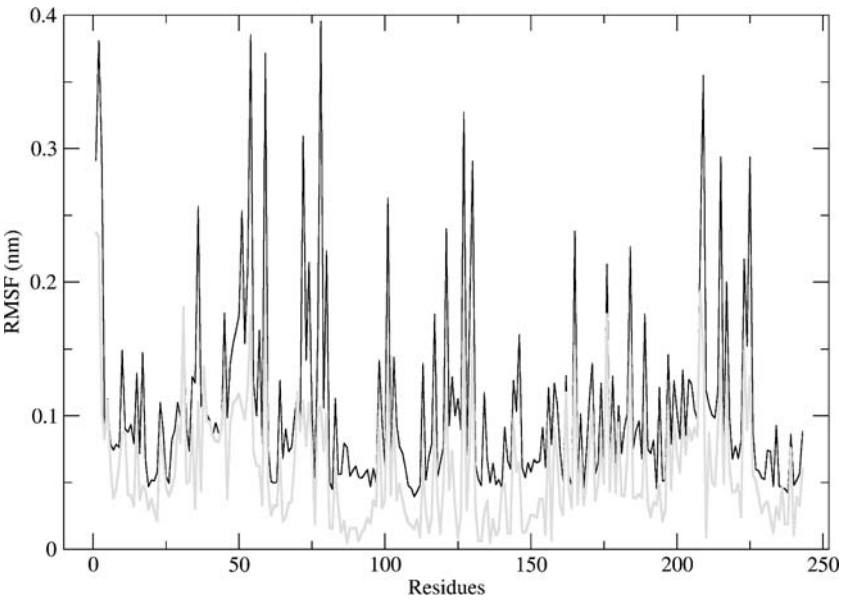

Fig. 5 Graphical representation of root-mean-square fluctuations (RMSF) of all Cα from starting structure of models as a function of time. The graphic shows the RMSF of uncomplexed PfPNP and of PfPNP:IMMH:SO4 complex. The average of last 4 ns of calculation gives in black line uncomplexed PfPNP and gray line shows PfPNP:IMMH: SO4 complex

Table 1 Hydrogen bonds and hydrophobic contacts of PfPNP with IMMH of monomer A during MD simulation

Time	Hydrogen bond			Hydrophobic contact
	Residues(Chain)	Atoms	Distance (Å)	Residues(Chain)
Initial structure	Ser91(A)	OG→N4'	3.3	Cys92(A)
	Met183(A)	N→O2'	2.8	Tyr160(A)
	Glu184(A)	OE1→O2'	2.9	Trp212(A)
		OE1→O3'	3.2	
		OE2→O3'	3.1	
	Asp206(A)	OD1→N7	2.8	
	His7(B)	NE2→O5'	2.8	
1 ns	Ser91(A)	O→O2'	2.8	Met183(A)
		O→O3'	3.1	Trp212(A)
	Arg88(A)	NH2→O3'	3.1	
	Tyr160(A)	OH→N4	3.3	
2 ns	Gly65(A)	O→O5'	3.2	Cys92(A)
	Ser91(A)	O→O2'	2.5	Met183(A)
		O→O3'	3.2	Trp212(A)
	Tyr160(A)	OH→N4'	3.1	
	Glu184(A)	OE1→O5'	2.6	
3 ns	Ser91(A)	O→O2'	2.8	Met183(A)
		O→O3'	2.9	Trp212(A)
				Tyr160(A)
4 ns	Ser91(A)	O→O2'	3.1	Tyr160(A)
		O→O3'	3.3	Val181(A)
	Met183(A)	OE1→N1	2.8	
		SD→O5'	3.4	
	Met159(A)	O→N1	3.2	
5 ns	Ser91(A)	O→O2'	2.7	Cys92(A)
		O→O3'	3.4	Met183(A)
	Met159(A)	O→N1'	3.2	Trp212(A)

of this figure indicates that the uncomplexed structure (system 1) presents higher RMSD when compared with the structure of the complexed structure (system 2). In both systems the RMSD of C-alpha atoms after a rapid increasing show a relative stability during overall MD simulation, achieving a plateau between 2.0 and 2.5 Å, suggesting that 5 ns of unrestrained simulation was sufficient for stabilizing PfPNP and PfPNP:IMMH:SO4 structures.

Accordingly, the PfPNP:IMMH:SO4 complex structure appears to be slightly more stable than the ligand-free form of the enzyme as shown in Fig. 4, which suggests a slightly compacting process due to the presence of IMMH and sulfate ions.

Superposition of the average structure of PfPNP:IMMH:SO4 with the initial model (data no shown) does not show major conformational changes from the initial structure, which is consistent with the relatively low RMSD value. System 1 presents higher RMSD values, however its secondary structure was kept, and these high values are due to the flexibility of the uncomplexed form of PfPNP.

The flexibilities of the proteins were assessed by the RMSF values from MD of the trajectory which reflects the flexibility of each atom residue in a molecule (Fig. 5). The major backbone fluctuation occurs in the loop region and in the region surrounding the beta-alpha-beta fold, whereas regions with the low RMSF correspond exclusively to the rigid beta-alpha-beta fold. These results indicate the stability of structures in aqueous solution. In Fig. 5 we can observe higher flexibility in PfPNP in the loops regions constituted by residues 219–222 and 159–169 in relation of the complex PfPNP:IMMH:SO4. These loops are responsi-

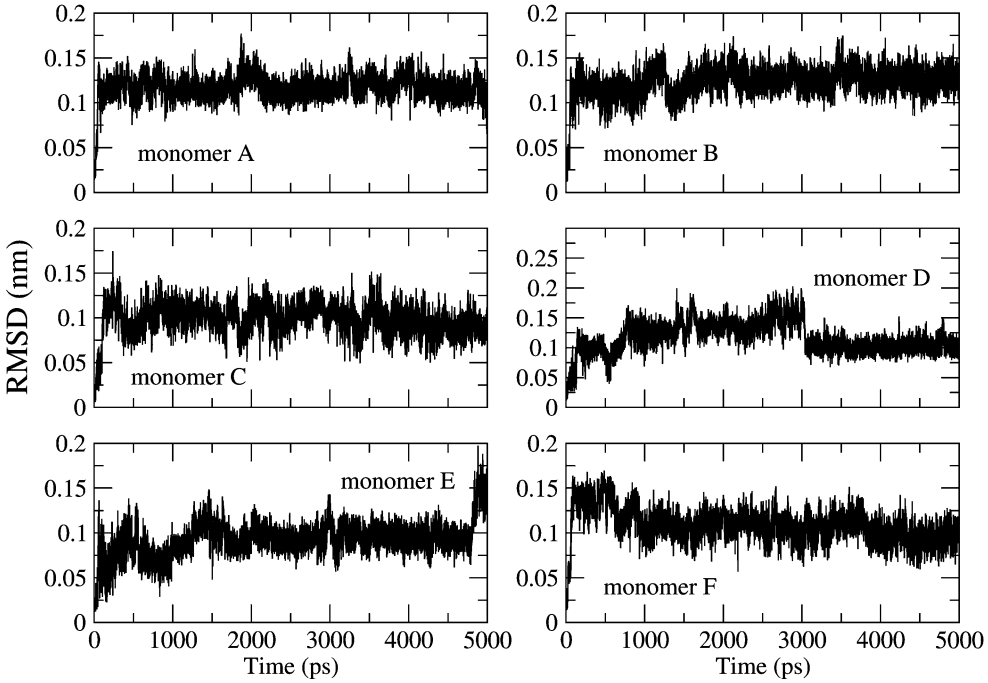

Fig. 6 Graphical representation of root-mean-square deviation (RMSD) of each IMMH structure from starting structure of monomers as a function of time

ble for substrate entrance and exit, as has been observed in the human PNP [24–36], and the flexibility is responsible to structural movement due to ligand binding.

Interaction of PfPNP with IMMH

The specificity and affinity between enzyme and its inhibitor depend on directional hydrogen bonds and ionic interactions, as well as on shape complementarity of the contact surfaces of both partners [37–53]. Analysis of the hydrogen bonds between PfPNP and IMMH reveals seven intermolecular hydrogen bonds. The residues involved in the interaction with IMMH and its length are shown in Table 1.

Along simulation of 5 ns the residues which make intermolecular hydrogen bond and hydrophobic contacts changes significantly, however some residues keep in contact with IMMH. The Ser91, Tyr160, and Glu184 maintained associated with IMMH at most part of MD by hydrogen bond or hydrophobic contact.

In despite of relative high flexibility of purine binding site, the IMMH presents a conformational stability into binding pocket (in Fig. 6 is shown the RMSD of IMMH). This stability suggests that designing of IMMH analogues and addition of chemical groups may improve electrostatic interactions with residues in the purine binding site.

Phosphate/sulfate-binding site

In the PNP:IMMH:SO4 structure, residues Gly23, Arg88, Ser91, and Arg45 of adjacent subunit form intermolecular hydrogen bonds with the sulfate bound close to the inhibitor. It was observed that the phosphate/sulfate-binding site keeps the same interactions with sulfate ions over MD simulations, suggesting that is a more stable than purine-binding site. In light of this observation, phosphate/sulfate binding site could become an alternative site for design of new inhibitors as observed by Timmers and co-workers [24] in human purine nucleoside phosphorylase (HsPNP).

Conclusions

This is the first report of a molecular dynamics simulation for a hexameric PNP. Molecular dynamics simulations of trimeric PNPs [24] has been previously reported. We focused our simulation studies on PNP from *Plasmodium falciparum*, due to its importance as a target for antimalarial drug development. The simulation of this hexameric structure brings new information about structural stability and PNP:IMMH interactions. IMMH is a transition state inhibitor with K_i in the picomolar range, which raises a problem due to its high affinity for human PNP. Therefore development of IMMH analogues with more selective activity will be the only way for the development of PfPNP inhibitor. The determination of interactions along the time in aqueous solutions could guide the process of designing or searching through virtual screening of new potential ligands. Identification of intermolecular interactions involving residues Gly23, Arg88, Ser91, and Arg45 of adjacent subunit completes the view of the active site that should be addressed in molecular docking simulations. In addition, the data

presented here suggest the mode of action for IMMH, with the conformational changes of the substrate binding loop involved in substrate entrance and exit, clearly seen when we compare molecular dynamics trajectories of both systems, ligand-free form (system 1) and complexed (system 2).

The phosphate/sulfate binding site has low mobility when complexed with sulfate and higher motion in ligand-free form, based on this observation we propose that this region is more stable when compared with purine binding site. Furthermore, the experimental studies could demonstrate that an alternative site can be useful for design of inhibitors.

Acknowledgments This work was supported by grants from CNPq (Conselho Nacional de Pesquisas, Brazil), CAPES and Instituto do Milênio (CNPq-MCT). RAC would like to thank CNPq for the fellowship. WFA and RGS are senior researchers of CNPq

References

1. Gilles HM (2002) In: Warrell DA, Gilles HM (eds) Essential Malariology. Arnold, New York, pp 1–7
2. World Health Organization (2007) Malaria, Fact Sheet No. 94. Geneva, Switzerland
3. Suh KN, Kain KC, Keystone JS (2004) Malaria. Can Med Assoc J 170:1693–1702
4. Sachs JD (2002) A new global effort to control malaria. Science 298:122–124
5. Wellems TE (2002) Plasmodium chloroquine resistance and the search for a replacement antimalarial drug. Science 298:124–125
6. Hassan HF, Coombs GH (1988) Purine and pyrimidine metabolism in parasitic protozoa. FEMS Microbiol Rev 4:47–83
7. Asahi H, Kanazawa T, Kajihara Y, Takahashi K, Takahashi T (1996) Hypoxanthine: a low molecular weight factor essential for growth of erythrocytic Plasmodium falciparum in a serum-free medium. Parasitology 113:19–23
8. Kicska GA, Tyler PC, Evans GB, Furneaux RH, Kim K, Schramm VL (2002) Transition state analogue inhibitors of purine nucleoside phosphorylase from Plasmodium falciparum. J Biol Chem 277:3219–3225
9. Kicska GA, Tyler PC, Evans GB, Furneaux RH, Schramm VL, Kim K (2002) Purine-less death in Plasmodium falciparum induced by immucillin-H, a transition state analogue of purine nucleoside phosphorylase. J Biol Chem 277:3226–3231
10. Ting LM, Shi W, Lewandowicz A, Singh V, Mwakingwe A, Birck MR, Ringia EA, Bench G, Madrid DC, Tyler PC, Evans GB, Furneaux RH, Schramm VL, Kim K (2005) Targeting a novel Plasmodium falciparum purine recycling pathway with specific immucillins. J Bio Chem 280:9547–9554
11. Schnick C, Robien MA, Brzozowski AM, Dodson EJ, Murshudov GB, Anderson L, Luft, Mehlin C, Hol WGJ, Brannigan JA, Wilkinson AJ (2005) Structures of Plasmodium falciparum purine nucleoside phosphorylase complexed with sulfate and its natural substrate inosine. Acta Crystallogr D Biol Crystallogr 61:1245–1254
12. Shi W, Ting LM, Kicska GA, Lewandowicz A, Tyler PC, Evans GB, Furneaux RH, Kim K, Almo SC, Schramm VL (2004) Plasmodium falciparum purine nucleoside phosphorylase. J Biol Chem 279:18103–18106
13. Berman HM, Battistuz T, Bhat TN, Bluhm WF, Bourne PE, Burkhardt K, Feng Z, Gilliland GL, Iype L, Jain S, Fagan P, Marvin J, Padilla D, Ravichandran V, Schneider B, Thanki N, Weissig H, Westbrook JD, Zardecki C (2002) The Protein Data Bank. Acta Crystallogr D Biol Crystallogr 58:899–907
14. van der Spoel D, Lindahl E, Hess B, Groenhof G, Mark AE, Berendsen HJC (2005) GROMACS: fast, flexible, and free. J Comp Chem 26:1701–1718 http://www.gromacs.org
15. Ooestenbrink C, Soares TA, van der Vegt NF, van Gunsteren WF (2005) Validation of the 53A6 GROMOS force field. Eur Biophys J 34:273–284
16. van Aalten DM, Bywater B, Findlay JB, Hendlich M, Hooft RW, Vriend G (1996) PRODRG, a program for generating molecular topologies and unique molecular descriptors from coordinates of small molecules. Comput Aided Mol Des 10:255–262 http://davapc1.bioch.dundee.ac.uk/programs/prodrg/prodrg.html
17. Schmidt MW, Baldridge KK, Boatz JA, Elbert ST, Gordon MS, Jensen JH, Koseki S, Matsunaga N, Nguyen KA, Su S, Windus TL, Dupuis M, Montgomery JA (1993) General atomic and molecular electronic structure system. J Comput Chem 14:1347–1363
18. Guex N, Peitsch MC (1997) SWISS-MODEL and the Swiss-PdbViewer: an environment for comparative protein modeling. Electrophoresis 18:2714–2723
19. Berendsen HJC, Postma JPM, van Gunsteren WF, Hermans J (1981) Interaction models for water in relation to protein hydration. In: Pullman B (ed) Intermolecular forces. Reidel D Publishing Company Dordrecht, The Netherlands, pp 331–342
20. Hess B, Bekker H, Berendsen HJC, Fraaije JGEM (1997) LINCS: a linear constraint solver for molecular simulations. J Comput Chem 18:1463–1472
21. Miyamoto S, Kollman PA (1992) Absolute and relative binding free energy calculations of the interaction of biotin and its analogs with streptavidin using molecular dynamics/free energy perturbation approaches. J Comput Chem 16:226–245
22. Chowdhuri S, Tan ML, Ichiye T (2006) Dynamical properties of the soft sticky dipole-quadrupole-octupole water model: a molecular dynamics study. J Chem Phys 125:144513
23. Darden T, York D, Pedersen L (1993) Particle Mesh Ewald - an n. log(n) method for ewald sums in large systems. J Chem Phys 98:10089–10092
24. Timmers LFSM, Caceres RA, Vivan AL, Gava LM, Dias R, Ducati RG, Basso LA, Santos DS, de Azevedo WF (2008) Structural studies of human purine nucleoside phosphorylase: towards a new specific empirical scoring function. Arch Biochem Biophys 479:28–38
25. Silva RG, Nunes JE, Canduri F, Borges JC, Gava LM, Moreno FB, Basso LA, Santos DS (2007) Purine nucleoside phosphorylase: a potential target for the development of drugs to treat T-cell- and apicomplexan parasite-mediated diseases. Curr Drugs Target 8:413–422
26. de Azevedo WF Jr, Canduri F, dos Santos DM, Silva RG, de Oliveira JS, de Carvalho LPS, Basso LA, Mendes MA, Palma MS, Santos DS (2003) Crystal structure of human purine nucleoside phosphorylase at 2.3 Å resolution. Biochem Biophys Res Commun 308:545–552
27. Caceres RA, Saraiva Timmers LF, Dias R, Basso LA, Santos DS, de Azevedo WF (2008) Molecular modeling and dynamics simulations of PNP from Streptococcus agalactiae. Bioorg Med Chem 16:4984–4993
28. Timmers LFSM, Caceres RA, Basso LA, Santos DS, de Azevedo Jr. WF (2008) Structural Bioinformatics Study of PNP from Listeria monocytogenes. Protein Pep Lett 15:843–849
29. de Azevedo WF Jr, Canduri F, dos Santos DM, Pereira JH, Dias MVB, Silva RG, Mendes MA, Basso LA, Palma MS, Santos DS (2003) Structural basis for inhibition of human PNP by immucillin-H. Biochem Biophys Res Commun 309:917
30. Canduri F, Fadel V, Basso LA, Palma MS, Santos DS, de Azevedo WF (2005) New catalytic mechanism for human purine nucleoside phosphorylase. Biochem Biophys Res Commun 327:646–649

31. Santos DM, Canduri F, Pereira JH, Dias MVB, Silva RG, Mendes MA, Palma MS, Basso LA, de Azevedo WF, Santos DS (2003) Crystal structure of human purine nucleoside phosphorylase complexed with acyclovir. Biochem Biophys Res Commun 308:553–559
32. de Azevedo WF, Canduri F, dos Santos DM, Pereira JH, Dias MVB, Silva RG, Mendes MA, Basso LA, Palma MS, Santos DS (2003) Crystal structure of human PNP complexed with guanine. Biochem Biophys Res Commun 312:767–772
33. Silva RG, Pereira JH, Canduri F, de Azevedo WF, Basso LA, Santos DS (2005) Kinetics and crystal structure of human purine nucleoside phosphorylase in complex with 7-methyl-6-thio-guanosine. Arch Biochem Biophys 442:49–58
34. Canduri F, dos Santos DM, Silva RG, Mendes MA, Basso LA, Palma MS, de Azevedo WF, Santos DS (2004) Structures of human purine nucleoside phosphorylase complexed with inosine and ddI. Biochem Biophys Res Comum 313:907–914
35. Canduri F, Silva RG, dos Santos DM, Palma MS, Basso LA, Santos DS, de Azevedo WF(2005) Structure of human PNP complexed with ligands. Acta Crystallogr D Biol Crystallogr 61:856–862
36. Nolasco DO, Canduri F, Pereira JH, Cortinóz, Palma MS, Oliveira JS, Basso LA, de Azevedo WF, Santos DS (2004) Crystallographic structure of PNP from Mycobacterium tuberculosis at 1.9 Å resolution. Biochem Biophys Res Comum 324:789–794
37. de Azevedo WF, Dias R (2008) Computational methods for calculation of ligand-binding affinity. Curr Drug Targets 9:1031–1039
38. de Azevedo WF (2008) Protein-drug interactions. Curr Drug Targets 9:1030–1030
39. Dias R, de Azevedo WF (2008) Molecular docking algorithms. Curr Drug Targets 9:1040–1047
40. Canduri F, de Azevedo WF (2008) Protein crystallography in drug discovery. Curr Drug Targets 9:1048–1053
41. Pauli I, Timmers LFSM, Caceres RA, Soares MBP, de Azevedo WF (2008) In silico and in vitro. Identifying new drugs. Curr Drug Targets 9:1054–1061
42. Dias R, Timmers LFSM, Caceres RA, de Azevedo WF (2008) Evaluation of molecular docking using polynomial empirical scoring functions. Curr Drug Targets 9:1062–1070
43. de Azevedo WF, Dias R (2008) Experimental approaches to evaluate the thermodynamics of protein-drug interactions. Curr Drug Targets 9:1071–1076
44. Caceres RA, Pauli I, Timmers LFSM, de Azevedo WF (2008) Molecular recognition models: a challenge to overcome. Curr Drug Targets 9:1077–1083
45. Barcellos GB, Pauli I, Caceres RA, Timmers LFSM, Dias R, de Azevedo WF (2008) Molecular modeling as tool for drug discovery. Curr Drug Targets 9:1084–1091
46. Timmers LFSM, Pauli I, Caceres RA, de Azevedo WF (2008) Drug-binding databases. Curr Drug Targets 9:1092–1099
47. de Azevedo WF , Canduri F, Fadel V, Teodoro LG, Hial V, Gomes RA (2001) Biochem Biophys Res Commun 287:277–281
48. de Azevedo WF (2007) Editorial. Current Drug Targets 8:387–387
49. Canduri F, Perez PC, Caceres RA, de Azevedo WF (2007) Protein kinases as targets for antiparasitic chemotherapy drugs. Curr Drug Targets 8:389–398
50. Marques MR, Pereira JH, Oliveira JS, Basso LA, Santos DS, de Azevedo WF , Palma MS (2007) The inhibition of 5-enolpyruvylshikimate-3-phosphate synthase as a model for development of novel antimicrobials. Curr Drug Targets 8:445–457
51. Dias MVB, Ely F, Palma MS, de Azevedo WF, Basso LA, Santos DS (2007) Chorismate synthase: an attractive target for drug development against orphan diseases. Curr Drug Targets 8:437–444
52. Pereira JH, Vasconcelos IB, Oliveira JS, Caceres RA, de Azevedo WF , Basso LA, Santos DS (2007) Shikimate kinase: a potential target for development of novel antitubercular. Curr Drug Targets 8:459–468
53. de Amorim HLN, Caceres RA, Netz PA (2008) Linear Interaction Energy (LIE) method in lead discovery and optimization. Curr Drug Targets 9:1100–1105